

## ADVANCED SOLUTIONS FOR CHEMICAL INACTIVATION AND SAFE DISPOSAL OF SLUDGE AFTER TREATING LIQUID WASTE

Ovidiu-Dorin ALUPEI-COJOCARIU<sup>1</sup>, Alexandra BANU<sup>2</sup>, Manuela Roxana DIJMĂRESCU<sup>3</sup>, Dragoș-Ştefan PREDA<sup>4</sup>, Elena RUSU<sup>5</sup>, Petrișor-Zamora IORDACHE<sup>6</sup>

*An advanced solution for chemical inactivation and safe disposal of sludge after treating liquid waste was investigated. A previously reported material is used for chemical inactivation of sludge under low-temperature thermolysis conditions. The sludge inactivation byproducts at 350°C are capable of completely fixing the heavy metals and significantly reducing the level of dissolved organic carbon, sulfates, and fluorides, below 1000 mg/kg SU, 500 mg/kg SU, and 1 mg/kg SU respectively. One of the main mechanisms undertaking chemical inactivation of waste having complex contamination is chemical condensation which gives rise to new materials with reduced chemical functionality and high chemical stability, such as for example, mineral oxysalts.*

**Keywords:** leachate, waste, liquid waste, waste disposal, waste treatment technologies, sludge, waste chemical inactivation

### 1. Introduction

Solving the sludge arising from liquid waste treatment processes is the thorniest technical challenge in the whole sector of liquid waste treating due to the severe deficit of feasible applied treatment solutions [1], but by far, the most problematic of all of them is the almost complete absence of the technical solutions to solve toxicity of wet waste after dewatering [2]. The few existing technical solutions in the field are limited to solving at great costs only some particular types of waste, such as for example, the composting of biodegradable waste released from domestic activities and farms. In addition, current technical solutions in the waste sludge field are totally eclipsed by the shortage in

<sup>1</sup> Assoc. Prof., Dept. of Manufacturing Engineering, National University for Science and Technology POLITEHNICA Bucharest, Romania, e-mail: ovidiu.alupei@gmail.com

<sup>2</sup> Prof., Dept. of Manufacturing Engineering, National University for Science and Technology POLITEHNICA Bucharest, Romania, e-mail: alexandrabanu14@yahoo.com

<sup>3</sup> Lecturer, National University for Science and Technology POLITEHNICA Bucharest, Romania, e-mail: manuela-d@live.com

<sup>4</sup> Eng., GREEN WATERNANOTECHNOLOGY, Bucharest, Romania, e-mail: darck.ro14@gmail.com

<sup>5</sup> Eng., GREEN WATERNANOTECHNOLOGY, Bucharest, Romania, e-mail: office@greenwaternanotechnology.ro

<sup>6</sup> Phys., GREEN WATERNANOTECHNOLOGY, Bucharest, Romania, e-mail: iordachezamora1978@gmail.com

technological progress which persists in all other sectors giving rise to wet waste, such as for example, the wet waste arising from industrial sectors, or those with radioactive or hazardous biological charge [3].

Finding solutions to transform simultaneously and in one stage a vast variety of hazardous contaminants from wet waste into chemically inactivated solid substrates is the supreme solution in the above-said field by that it supposes the ending of the waste life-cycle in one cyclic, sustainable, and endless way, for example, by transforming a wet waste into a fertile soil. Solutions such as chemical fixation, solidification, neutralization, and incineration can be used before disposing the hazardous wet wastes [4,5]. These solutions transform the toxic waste into more inert forms either by transforming some of its contaminants into less toxic ones or by reducing the total amount of waste. The waste characteristics which, among other things, include the physical, radioactive, chemical, biodegradability, hazardous degree, and toxicity features, typically decide the selection of the most effective disposal solution. The waste initialization before disposal involves waste pretreating before disposal which most often may include one or more solutions selected among volume reduction, chemical stabilization, degradation, segregation, and encapsulation [6,7].

Presently incineration is the best method allowing the gain of up to 60% reduction in waste volume reduction, wherein most contaminants can be totally destroyed except for small amounts [8]. When used in disposal, the incineration helps to reduce the sludge volume by turning waste into ash residues which are easy to handle for final disposal, but typically give rise to soluble species of toxic metal oxides. Chemical stabilization [9] involves the addition of chemicals to reduce the mobility of contaminants thus helping in the stabilization and solidification of hazardous waste contaminants; it is a cheap method wherein the chemicals are mixed with waste sludge, then the resulting mixture is pumped onto land to solidify under weathering conditions during a few weeks. Some solutions are used for chemical degradation of wastes, such as for example, oxidation, chlorination, and hydrolysis, but none of the above solutions can be effective when used separately; for example, hydrolysis proves to be an effective solution in degrading only carbamate and organophosphorus pesticides [10,11]. Through segregation, the waste is sorted based on chemical characteristics to avoid unnecessary transformations onto landfills [12]. Some wastes that cannot be detoxified may be confined into materials such as concrete and plastics before their disposal, but for small amounts steel barrels are good options for storage.

Disposal within adjacent water bodies is treated as temporary as well as permanent storage components [13]. By subsurface leaching, the liquid waste is pumped into underground cavities wherein waste is naturally treated when it passes through different strata of the soil [14]; the main drawbacks of these solutions are represented by spreading soluble hazardous contaminants into

underground water bodies and hence, by their long-term adverse effects induced to environment components by their fate and toxicity. Electro-osmosis dewatering and advanced electro-dewatering technologies may increase the content of dry matter in sludge from 20-25% up to around 40-45% when agriculture or incineration are preferred routes of disposal [15].

The disposal costs are the main drawbacks limiting waste disposal, wherein for example, the landspreading of solid and semi-solid sludge entails the lowest average costs (from €110 to about €160 on ton of disposed dry matter), and landfilling, mono-incineration, and co-incineration entails highest average costs (from €260 to about €350 on ton of disposed dry matter); but however, finding viable applied solutions for waste sludge detoxication is still the most challenging issue due to strict environment regulations [16]. The sludge composting costs range from €125 to about €600 on ton of dry sludge [17]. Dry matter content for agriculture use should be from 20% to about 45%. As for incineration, the dry matter content should be at least around 30% to achieve self-sustained combustion at around 850°C [18]. For disposal applications throughout cement kilns, thermal drying is required to produce a "substitute solid fuel" with about 90% dry matter content.

Herein throughout this paper, we present the findings of investigating a low-temperature thermolytic solution that uses an advanced material for the chemical inactivation of dewatered sludge, wherein, the evidence indicates solid thermolysis byproducts may be disposed of as harmless soil substrates or as mineral fertilizers.

## 2. Experimental

### 2.1. Designing the thermolysis unit

The thermolysis chamber had a loading volume of 5 L and was executed to operate under oxygen-free conditions during the chemical inactivation of dewatered sludge; additionally, the thermolysis chamber was equipped with an automated induction heating coil, temperature control equipment, and an attached paddle mixer for homogenizing inactivation mixture. Several batches of dewatered sludge (water content of about 68 wt. %) were loaded in the thermolysis chamber: each loaded batch contained about 1 kg of dewatered sludge; separately, each batch was chemically inactivated at 250°C, 350°C, and 500°C; and, in addition, for each of the aforementioned sludge treatment temperatures, the time of chemical inactivation subject was 10, 15, and 20 minutes (for optimization). The inactivation mixture was made by adding an advanced material (prepared as reported elsewhere [19]) to dewatered sludge wherein, the weight ratio of wet sludge to composite material added to the inactivation mixture was 90:10. After forming, the inactivation mixture was loaded inside thermolysis chamber then chamber was closed.



Fig. 1. The design of thermolysis equipment: (a) thermolysis chamber; (b) the thermolysis chamber inside view; (c) the induction heating unit of the coil

Further on, separately for each loaded batch, the thermolysis chamber was heated to the above-specified temperature of chemical inactivation with an increasing rate of temperature of about 60°C per minute; then the temperature of the thermolysis chamber was kept constant during the entire time of chemical inactivation. The steam generated during thermal treatment was expelled through an open slit located on the cover of the sealing the chamber, then directed through a glass pipeline to a water-cooled heat exchanger where the smog was separated from water and settled on the cooled surfaces of the exchanger. Promptly after ending the inactivation time, the heating was stopped and, further on, the thermolysis chamber was opened and solid residues were removed and collected.

The wet sludge subject to chemical inactivation herein was extracted from one leachate which was sampled from a waste deposit. The procedure to treat the leachate and the method to form the wet sludge after treatment were extensively presented by authors in the previous number of U.P.B. Sci. Bull. Series B. At the end of the step forming the wet sludge, the aqueous sludge extracted was placed for 72 hours on a porous fiber glass membrane (0.45  $\mu$ m), producing 5.2 kg of dewatered sludge (water content about 68 wt. %) were obtained.

## 2.2. Analytical investigations

Morphochemical investigations were made by scanning electron microscopy using combined a VEGA III microscope, whereas the microanalysis investigations were performed using a QUANTAX 400 X-ray spectrometer. The spectrometric investigations were realized by Fourier-transform infrared spectroscopy using a FTIR-6300 (JASCO) equipment (FTIR) to assess the functional structure of solid byproducts after chemical inactivation. For thermogravimetry differential thermal analysis we used a Perkin Elmer Thermal Analyzer (STA) 6000 equipment with simultaneous analysis TG-DTA mode. The XRD Measurements were made by using a Rigaku SmartLab X-Ray Diffractometer (Cu:  $K_{\beta 1}=1.39217$  Å,  $K_{\alpha 1}=1.540598$  Å, Cu  $K_{\alpha 2}=1.544426$  Å). The optical images were taken by using the SAMSUNG Galaxy A12 32 GB Quad

Camera. Differential scanning calorimetry (DSC) investigations were made by using a Diamond DSC Perkin-Elmer with nitrogen purge at a heating rate of 10 K/min between 20 and 180°C. The thermal stability of all samples was studied by employing Thermogravimetric Analyzer Q50 (TA Instruments) under nitrogen atmosphere, from room temperature to 550°C with a heating rate of 10 K/min.

### 2.2.1 Thermogravimetric investigations of sludge before treatment

The sludge sample was held for 1 min at 30°C, then was heated from 30°C to 900°C at a speed of 10°C min<sup>-1</sup>. From thermogravimetric analysis is observed an important decrease in sample mass (about 68%) when the temperature ranges from 30°C to 140°C which is attributed to the loss of water. In the range from 140°C to 320°C is noticed a 3% decrease in mass which may be attributed to the processes transforming particular cationic oxo-hydroxides into corresponding more chemically condensed speciations such as, for example, their oxides. The total mass loss in the range from 320°C to 900°C is about 7%, additionally being noticed that the mass decreases relatively constant. When the temperature reaches 900°C, the remaining residue represents 22% of the initial mass of the sludge.

The DTA data are in excellent agreement with those obtained by thermogravimetric analysis. Thus, an endothermic peak corresponding to water evaporation is observed which has a maximum at 93°C. Moreover, the DTA data indicate another endothermic peak, which is much wider and less high when the temperature passes through the range 140-320°C.

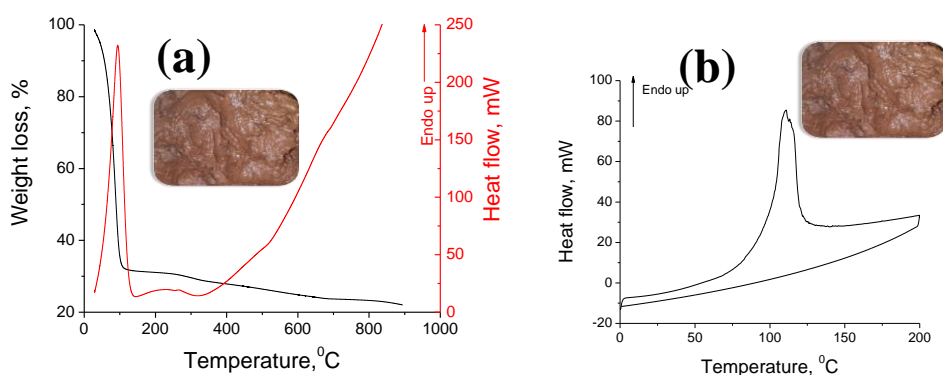


Fig. 2. The results of thermogravimetric lab investigations: (a) TG (black) and DTA (red); (b) DSC curve of sludge before undergoing chemical inactivation

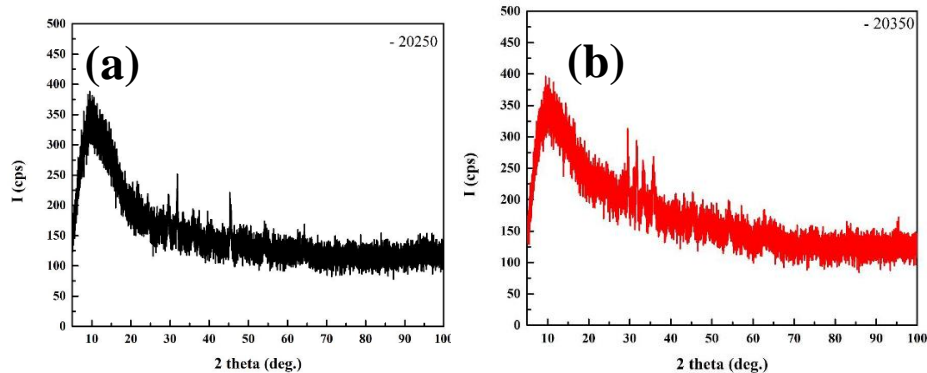
The maximum of the second DTA peak appears at 230°C, case wherein, we suspect that this was possible to arise through discrete transformations of particular aqua-oxo-hydroxylated phases into oxides. Since the water content in sludge is high (about 68%), therefore the peak corresponding to water evaporation is much higher compared to others.

The DSC investigations were made by heating the sample from 0 to 200°C at a rate of 10°C min<sup>-1</sup>, then this was cooled on the same temperature domain and at the same speed. Here as well can be noticed the endothermic effect of water evaporation with a maximum at about 110°C. Also, we notice that the water evaporation endothermic effect prevails and no other thermal effects were observed within the temperature range which was investigated through DSC. The second heating-cooling cycle doesn't reveal the existence of other thermal effects.

### 2.2.2 XRD investigations to resolve the composition of thermolysis chemically inactivated material

As shown in Fig. 6, the solid residues collected from the thermolysis chamber are amorphous solid material mixtures in the form of dust.

The composition of solid byproducts collected after chemical inactivation of sludge at 250°C was solved by X-ray diffraction investigations (as shown in Fig. 3), case when the composition of inactivation byproducts is made of trisodium dipotassium triphosphidiosilicate (card 1008466), diopside (card 1000015), srebrodolskite (card 1008777), nepheline (card 1008753), potassium iron (III) diphosphate (card 1001388), magnesium chlorate (VII) hexahydrate (card 1000064), dicalcium magnesium disilicate (card 1010215), fayalite (card 1000064), sodium dioxoferrate (III)- $\beta$  (card 1008191), Al<sub>2</sub>O<sub>3</sub>-k (card 8103514), wherein  $2\theta_{250}$  appear at 8.52°, 12.31°, 24.39°, 29.64°, 31.84°, 33.26°, 35.9°, 45.44°, 54.4°, and 64.44°. The treatment byproducts collected when the sludge was chemically inactivated at 350°C have the same composition as those obtained when the sludge was inactivated at 250°C and 500°C, except that  $2\theta_{350}$  appear at 13.77°, 29.56°, 31.7°, 35.92°, 41.05°, 45.53°, 54.24°, and 62.77°, and  $2\theta_{500}$  appear at 9.66°, 31.74°, 35.62°, 62.7°, and 114.55°. Also, we found that smog which was collected after the chemical inactivation of sludge at 350°C for 20 min. (Fig.3(d)) has the same composition as the inactivation byproducts obtained when the sludge was inactivated at 250°C, 350°C, and 500°C, except that smog does not contain sodium dioxoferrate (III)- $\beta$ , and  $2\theta_{smog}$  appear at 8.32°, 29.5°, 31.77°, 33.27°, 35.79°, 39.7°, 43.4°, 45.54°, 47.49°, 48.66°, 54.22°, 62.66°, and 84.03°.



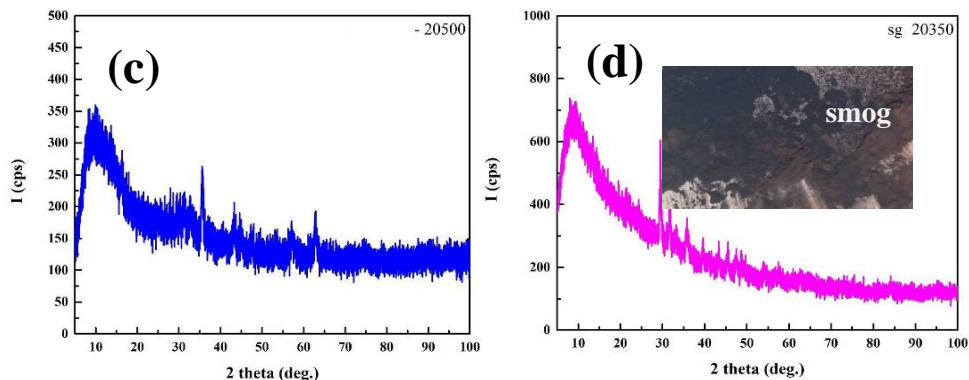


Fig. 3. The X-ray diffraction spectra of treatment byproducts resulting after sludge inactivation at (a) 250°C for 20 min., (b) 20 min for 350°C, (c) 20 min for 500°C; (d) smog collected after inactivation treatment made at 350°C for 20 min.

### 2.2.3 FTIR investigations of chemically inactivated material

Essentially, the chemical condensation made under thermolysis conditions consists of eliminating the aquo ligands and hydroxo ligands from the structure of aquo-oxo-hydroxylated components. Examples of ligands associated with forming condensed components during chemical condensation include, for example, components bonding hydroxo ligands which may be associated with the formula M-OH, or components containing "ol" bridges M-OH-M associated with formula  $x(OH)_y$  arising by condensing the ligands -OH and  $(OH_2)$  of aquo-hydroxylated components of advanced material wherein, "x" is number of metal atoms linked by one "ol" bridge and "y" is the number of bridges between these "x" and the metal atoms wherein, typically "x" is 1 or 2; also herein are included, for example, species bonding or containing one or more strong bonds of oxo =O ligands which may arise through condensing the hydroxo groups of hydroxylated contamination components, wherein such speciations possess the highest chemical stability.

The experimental evidence gained by FTIR are in excellent agreement with those obtained by TG, DTA, DSC, and XRD, indicating that during thermolysis, the inactivation admixture undergoes advanced chemical condensation processes through which the advanced material charged with captured contaminants is transformed into more condensed solid material fractions which mainly contain mixtures of oxides and aquo-oxo-hydroxylated cationic salts emanating from the advanced material, as well carbonized fractions arriving from organic contaminants degradation.

Both figures Fig. 4 and Fig. 5 clearly indicate the water is removed quickly and the removed amount rises gradually as the temperature and thermolysis time increase. At 500°C, the IR spectra show a clear distinctive structure of its peaks which indicates these are emanated by a material with a more discreet structure, reason way therefore we suspect they belong to trisodium dipotassium triphosphidiosilicate, diopside, srebrodolskite, nepheline, potassium

iron(III) diphosphate, magnesium chlorate(VII) hexahydrate, dicalcium magnesium disilicate, fayalite, sodium dioxoferrate(III)- $\beta$ , Al<sub>2</sub>O<sub>3</sub>-k, and derived chemical speciations of the below.

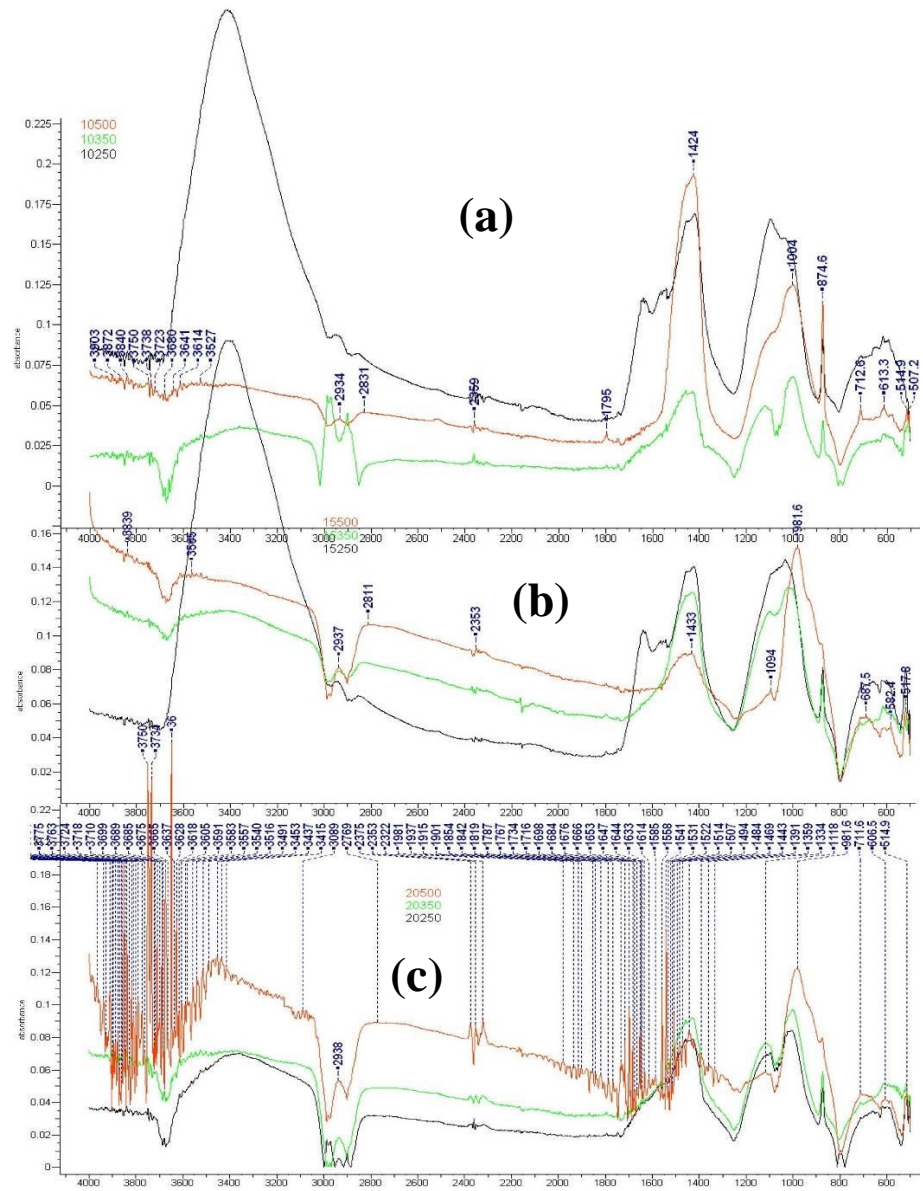


Fig. 4. Overlapped FTIR spectra of byproducts obtained after sludge inactivation for (a) 10 min. (at 250°C – 10250, 350°C – 10350, 500°C – 10500), (b) 15 min. (at 250°C – 15250, 350°C – 10350, 500°C – 10500), and (c) 20 min. (at 250°C – 20250, 350°C – 20350, 500°C – 20500)

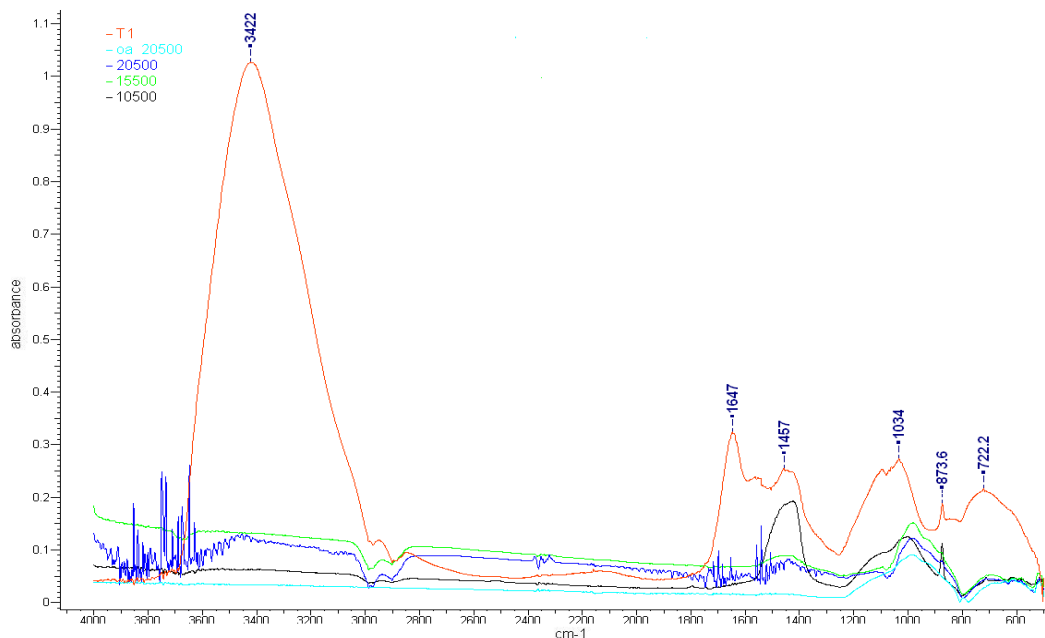


Fig. 5. The overlapped FTIR spectra of sludge before treatment (red T1); sludge chemical inactivation byproducts formed at 500°C and 10 min. (label oa 20500), under open-air thermolysis conditions (open thermolysis chamber); and sludge chemical inactivation byproducts formed at 500°C and 10 min. (label 15500), 15 min. (label 20500), respectively 20 min.

For example, the adsorption profiles in Fig. 4 and Fig. 5 corresponding to inactivation conditions at 500°C for 20 minutes (marked as 20500) indicate the presence of  $\mu_3$ -OH intercrystalline bonded by three metal cations ( $3718\text{ cm}^{-1}$ ),  $\mu_2$ -OH intercrystalline bonded by two metal cations (around  $3710\text{ cm}^{-1}$ ),  $\nu(\text{OH})$  bands (around  $3699\text{ cm}^{-1}$ ),  $\nu_{\text{as}}(\text{OH})$  and  $\nu_{\text{s}}(\text{OH})$  of  $\text{H}_2\text{O}$  adsorbed on open metal sites and hydroxyl groups in metal-organic framework (around  $3591\text{ cm}^{-1}$ ,  $3557\text{ cm}^{-1}$ ,  $3542\text{ cm}^{-1}$ ,  $3450\text{ cm}^{-1}$ ),  $\nu_{\text{s}}(\text{OH})$  of water coordinated to cationic charged sites (around  $3582\text{ cm}^{-1}$ ,  $3415\text{ cm}^{-1}$ ),  $\nu_{\text{as}}$  and  $\nu_{\text{s}}$  modes of water adsorbed on the OH groups (around  $3540\text{ cm}^{-1}$ ),  $\text{NH}_2$ -related amino-functionalized metal-organic framework (around  $3516\text{ cm}^{-1}$ ,  $3491\text{ cm}^{-1}$ ,  $3437\text{ cm}^{-1}$ ,  $3415\text{ cm}^{-1}$ ), and C–H stretching modes arising from encapsulated trace organics (around  $3089\text{ cm}^{-1}$ ) [20].  $\text{CO}_2$  adsorbed on organic linkers in metal-organic framework, including those coordinated to cationic charged sites, appear around  $2322\text{ cm}^{-1}$ , and  $2353\text{ cm}^{-1}$  (most likely arising within thermal treatment). Additionally, the adsorption profile on the spectral domain from  $2000\text{ cm}^{-1}$  to  $500\text{ cm}^{-1}$  shows evidence of the presence of  $\text{M}^{2+}\text{-NO}$  species (around  $1854\text{ cm}^{-1}$ ,  $1842\text{ cm}^{-1}$ ,  $1819\text{ cm}^{-1}$ ,  $1787\text{ cm}^{-1}$ ,  $1767\text{ cm}^{-1}$ ,  $1734\text{ cm}^{-1}$ ),  $\nu_{\text{as}}(\text{C–O–C})$  (around  $1819\text{ cm}^{-1}$ ),  $\nu_{\text{s}}(\text{C=O})$  (around  $1787\text{ cm}^{-1}$ ,  $1767\text{ cm}^{-1}$ ,  $1767\text{ cm}^{-1}$ ,  $1734\text{ cm}^{-1}$ ,  $1716\text{ cm}^{-1}$ ,  $1698\text{ cm}^{-1}$ ,  $1684\text{ cm}^{-1}$ ,  $1653\text{ cm}^{-1}$ ), ammonium ions (around  $1734\text{ cm}^{-1}$ ,  $1676\text{ cm}^{-1}$ ,  $1734\text{ cm}^{-1}$ ,  $1676\text{ cm}^{-1}$ ,  $1494\text{ cm}^{-1}$ ), ammonia coordinated to cationic sites (around  $1644\text{ cm}^{-1}$ ,  $1644\text{ cm}^{-1}$ ).

$\text{cm}^{-1}$ , 1118  $\text{cm}^{-1}$ ),  $\nu(\text{P=O})$  (around 1734  $\text{cm}^{-1}$ , 1698  $\text{cm}^{-1}$ ), uncoordinated  $-\text{COOH}$  groups or unreacted  $\text{M}^{2+}-\text{NO}$  species (around 1854  $\text{cm}^{-1}$ , 1842  $\text{cm}^{-1}$ , 1819  $\text{cm}^{-1}$ , 1787  $\text{cm}^{-1}$ , 1767  $\text{cm}^{-1}$ , 1734  $\text{cm}^{-1}$ ),  $\nu_{\text{as}}(\text{C}-\text{O}-\text{C})$  (around 1819  $\text{cm}^{-1}$ ),  $\nu_{\text{s}}(\text{C=O})$  (around 1787  $\text{cm}^{-1}$ , 1767  $\text{cm}^{-1}$ , 1767  $\text{cm}^{-1}$ , 1734  $\text{cm}^{-1}$ , 1716  $\text{cm}^{-1}$ , 1698  $\text{cm}^{-1}$ , 1684  $\text{cm}^{-1}$ , 1653  $\text{cm}^{-1}$ ), ammonium ions (around 1734  $\text{cm}^{-1}$ , 1676  $\text{cm}^{-1}$ , 1494  $\text{cm}^{-1}$ ), ammonia coordinated to cationic sites (around 1644  $\text{cm}^{-1}$ , 1118  $\text{cm}^{-1}$ ),  $\nu(\text{P=O})$  (around 1734  $\text{cm}^{-1}$ , 1698  $\text{cm}^{-1}$ ), uncoordinated  $-\text{COOH}$  groups or unreacted  $\text{M}^{2+}-\text{NO}$  species (around 1854  $\text{cm}^{-1}$ , 1842  $\text{cm}^{-1}$ , 1819  $\text{cm}^{-1}$ , 1787  $\text{cm}^{-1}$ , 1767  $\text{cm}^{-1}$ , 1734  $\text{cm}^{-1}$ ),  $\nu_{\text{as}}(\text{C}-\text{O}-\text{C})$  (around 1819  $\text{cm}^{-1}$ ),  $\nu_{\text{s}}(\text{C=O})$  (around 1787  $\text{cm}^{-1}$ , 1767  $\text{cm}^{-1}$ , 1767  $\text{cm}^{-1}$ , 1734  $\text{cm}^{-1}$ , 1716  $\text{cm}^{-1}$ , 1698  $\text{cm}^{-1}$ , 1684  $\text{cm}^{-1}$ , 1653  $\text{cm}^{-1}$ ),  $\nu(\text{P=O})$  (around 1734  $\text{cm}^{-1}$ , 1698  $\text{cm}^{-1}$ ), uncoordinated  $-\text{COOH}$  groups or unreacted ligand molecules (around 1734  $\text{cm}^{-1}$ , 1716  $\text{cm}^{-1}$ , 1653  $\text{cm}^{-1}$ ),  $\text{C}-\text{O}$  bands (around 1716  $\text{cm}^{-1}$ ),  $\text{NO}_x$  adsorption on various cationic substrates (around 1698  $\text{cm}^{-1}$ , 1684  $\text{cm}^{-1}$ , 1633  $\text{cm}^{-1}$ ), carboxylate linkers in metal-organic framework (around 1698  $\text{cm}^{-1}$ , 1653  $\text{cm}^{-1}$ ),  $\text{NO}_2$  nitrates (around 1698  $\text{cm}^{-1}$ , 1666  $\text{cm}^{-1}$ , 1653  $\text{cm}^{-1}$ , 1644  $\text{cm}^{-1}$ , 1614  $\text{cm}^{-1}$ , 1531  $\text{cm}^{-1}$ , 1359  $\text{cm}^{-1}$ ),  $\nu_{\text{as}}(\text{COO}^-)$  (around 1684  $\text{cm}^{-1}$ , 1676  $\text{cm}^{-1}$ , 1666  $\text{cm}^{-1}$ , 1647  $\text{cm}^{-1}$ , 1644  $\text{cm}^{-1}$ , 1633  $\text{cm}^{-1}$ , 1614  $\text{cm}^{-1}$ , 1585  $\text{cm}^{-1}$ , 1585  $\text{cm}^{-1}$ , 1558  $\text{cm}^{-1}$ , 1541  $\text{cm}^{-1}$ , 1531  $\text{cm}^{-1}$ , 1522  $\text{cm}^{-1}$ , 1507  $\text{cm}^{-1}$ , 1443  $\text{cm}^{-1}$ , 1391  $\text{cm}^{-1}$ , 1359  $\text{cm}^{-1}$ , 1359  $\text{cm}^{-1}$ , 711  $\text{cm}^{-1}$ ), aliphatic  $\nu(\text{C=N})$  (around 1585  $\text{cm}^{-1}$ ),  $-\text{C=O}-\text{O}$  bonds (around 1585  $\text{cm}^{-1}$ ),  $\delta(\text{NH}_2)$  (around 1585  $\text{cm}^{-1}$ ),  $\delta(\text{N-H})$  (around 1507  $\text{cm}^{-1}$ ),  $\text{NH}_2$  species (around 1558  $\text{cm}^{-1}$ , 1507  $\text{cm}^{-1}$ ), inter-ring  $\text{C}-\text{C}$  stretching modes (around 1558  $\text{cm}^{-1}$ ),  $\nu_2(\text{CO}_2)$  bands (around 669  $\text{cm}^{-1}$ ),  $\nu(\text{C-C})_{\text{ring}}$  (around 1541  $\text{cm}^{-1}$ , 1522  $\text{cm}^{-1}$ , 1507  $\text{cm}^{-1}$ ),  $\nu(\text{C-C})$  (around 1514  $\text{cm}^{-1}$ , 1484  $\text{cm}^{-1}$ , 1469  $\text{cm}^{-1}$ ),  $\delta_{\text{s}}(\text{CH})$  ( $\nu_5$ ) (around 1391  $\text{cm}^{-1}$ , 1318  $\text{cm}^{-1}$ ),  $\nu_{\text{as}}(\text{SO}_2)$  (around 1359  $\text{cm}^{-1}$ ),  $\nu(\text{O-O})$  (around 1118  $\text{cm}^{-1}$ ),  $\text{M}_2-\text{OH}$  (around 1118  $\text{cm}^{-1}$ ), incorporated sulfates and physisorbed  $\text{SO}_2$  species on  $\text{M}^{3+}$  sites (around 1118  $\text{cm}^{-1}$ ),  $\delta(\text{OH})$  (around 981  $\text{cm}^{-1}$ ),  $\text{M=O}$  (around 895  $\text{cm}^{-1}$ ),  $\text{M}-\text{O}-\text{M}$  (around 895  $\text{cm}^{-1}$ , 711  $\text{cm}^{-1}$ ),  $\text{M}-\text{O}$  modes (around 680  $\text{cm}^{-1}$ , 615  $\text{cm}^{-1}$ ),  $\text{M}-(\eta_2-\text{O}_2)$  (around 711  $\text{cm}^{-1}$ ),  $\text{M}-\text{X}$  sample a band at 680  $\text{cm}^{-1}$  (around 680  $\text{cm}^{-1}$ ),  $\nu_{\text{as}}(\text{M}_3\text{O})$  (around 606  $\text{cm}^{-1}$ ),  $\beta_{\text{s}}(\text{COO}^-)$  at 590–570  $\text{cm}^{-1}$ ,  $\text{S=O}$  deformation mode (around 515  $\text{cm}^{-1}$ ), and  $\mu_3-\text{OH}$  in various metal-organic framework (around 515  $\text{cm}^{-1}$ ) wherein, M is a cation forming the composition of advanced material as elsewhere reported [19].

However, we note that the adsorption profile in Fig. 5 which is specific to sludge inactivated under open-air thermolysis conditions is completely dissimilar from those of sludge inactivated in the absence of the air by that this presents relevant IR adsorption only on the spectral domain from about 1200  $\text{cm}^{-1}$  to 500  $\text{cm}^{-1}$  which typically are specific to inorganic fractions. These are strong evidence which indicates that a significant fraction of organic contaminants are released as superheat gaseous byproducts during open-air thermolysis; still, quantitative morphochemical EDX analyses indicate that other significant fraction of organic

contaminants is transformed into carbonaceous substrates which remain trapped inside of wet inactivation mixture formed in presence of advanced material.

Before chemical inactivation, the contaminated sludge contains a large variety of compounds whose chemical structure incorporates numerous types of chemical functionalities as described in more detail elsewhere [19]. The evidence herein shows that the composition of solid byproducts arising after chemical inactivation comprises a very limited number of compounds mainly consisting of trisodium dipotassium triphosphosilicate, diopside, srebrodolskite, nepheline, potassium iron(III) diphosphate, magnesium chlorate(VII) hexahydrate, dicalcium magnesium disilicate, fayalite, sodium dioxoferrate(III)- $\beta$ , and  $\text{Al}_2\text{O}_3\text{-k}$ , and speciations of the above. Additionally, we note that chemical inactivation byproducts pose a very limited chemical functionality comprising only a few specific types of chemical functionalities mainly consisting of mixtures of highly condensed mineral oxysalts.

#### 2.2.4 Morphostructural investigations

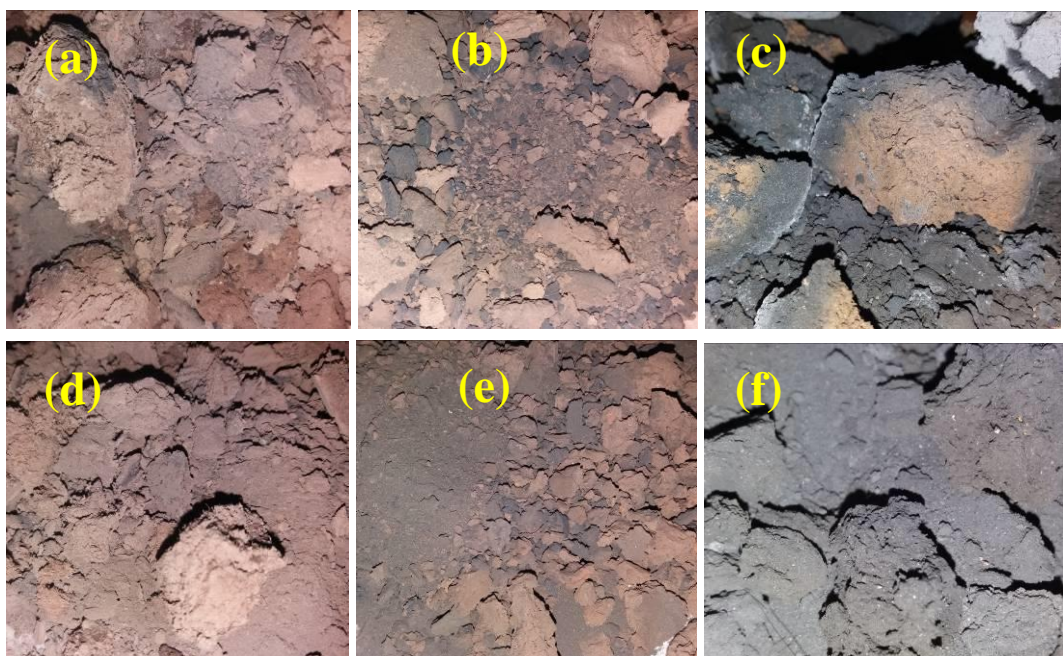
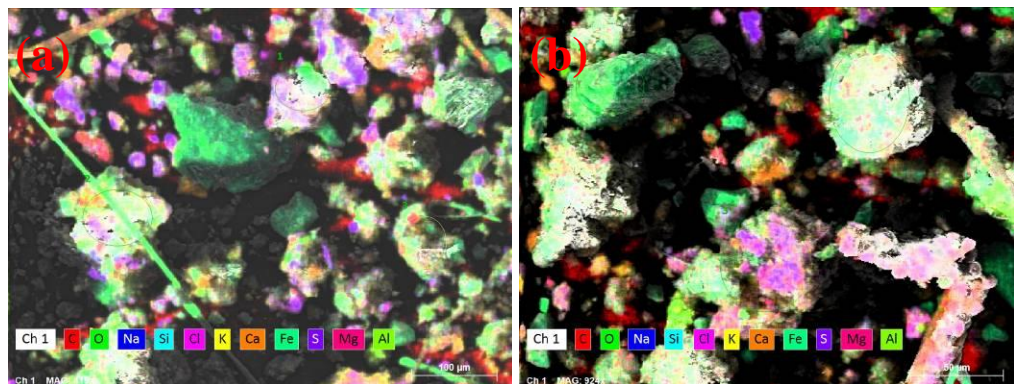




Fig. 6. Optical images of chemical-inactivated sludge after (a) 10 min at 250°C, (b) 10 min at 350°C, (c) 10 min at 500°C, (d) 15 min at 250°C, (e) 15 min at 350°C, (f) 15 min at 500°C, (g) 20 min at 250°C; (h) 20 min at 350°C, (i) 20 min at 500°C

The distribution profile of chemical functionalities revealed by the IR spectra herein indicates that organic contamination is reduced to salts of organic acids, sulfates, nitrates, and halides, as well as salts of ammonia and aminated and related aminated compounds. Furthermore, the EDX mapping analyses herein (Fig. 7 and Fig. 8) reveal that the organic contamination seem to be either incorporated, physisorbed, coordinated, or incorporated into the framework of above-mentioned mineral oxysalt minerals thus forming encapsulated metal-organic frameworks.



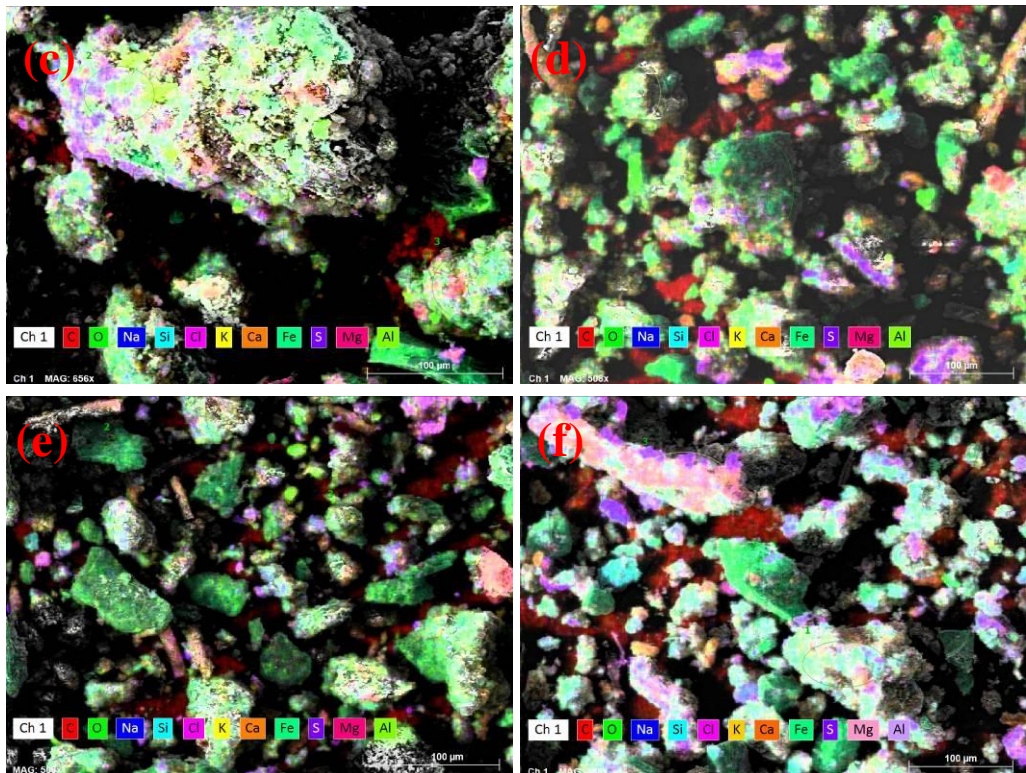


Fig. 7. Elemental EDX mapping made on chemical inactivated sludge obtained after: (a) 10 min at 250°C, (b) 10 min at 350°C, (c) 10 min at 500°C, (d) 15 min at 250°C, (e) 15 min at 350°C, (f) 15 min at 500°C

Consistent with data in Table 1, the quantitative elemental EDX analysis indicates that the mass percent of carbon trapped by chemically inactivated material ranges up to about 25.60%, based on the total mass percent amassing all chemical elements measured on the EDX maps in Fig. 8.

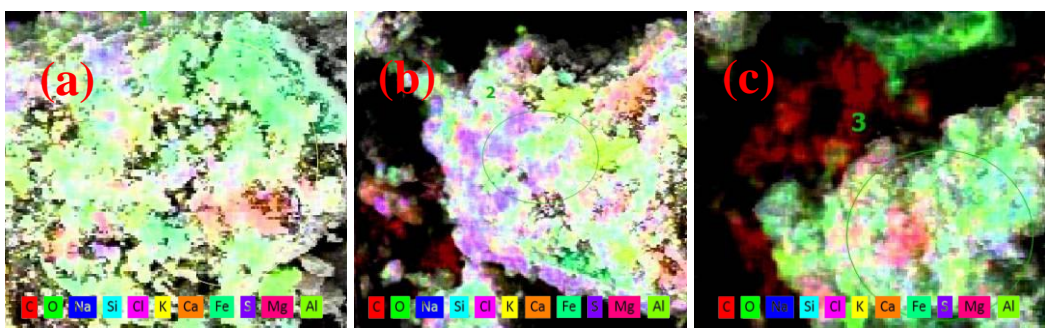


Fig. 8. Quantitative elemental EDX analysis made on three reference microsurfaces of chemically inactivated sludge at 500°C for 10 min.

This evidence indicates that during thermolysis the organic contaminants first are chemically degraded when they are gradually transformed up to carbonaceous substrates, then they trapped throughout mineral oxysalts fractions structure.

*Table 1*  
**Results of quantitative elemental analysis made on the three microsurfaces referenced in Fig. 8**

Measured element	Mass Norm. [%] on reference microsurface 1	Mass Norm. [%] on reference microsurface 2	Mass Norm. [%] on reference microsurface 3
Oxygen	38.64	41.30	43.46
Carbon	25.60	15.81	13.83
Iron	9.28	6.05	6.95
Calcium	8.57	8.05	11.60
Silicon	4.62	6.22	7.49
Sodium	4.26	6.80	4.78
Aluminum	3.97	5.89	5.47
Chlorine	2.41	5.30	2.21
Potassium	1.16	1.97	1.38
Magnesium	0.78	1.41	2.00
Sulfur	0.70	1.20	0.83

### 2.2.5 Leaching investigations

Since during thermolytic inactivation of sludge it was observed that the type of mineral phases forming the final composition of chemically inactivated sludge remain the same, we may naturally conclude there is a point in the sludge transformation temperature at which the sludge composition components start to nucleate and to form mineral phases which therefore, later form the composition of chemical inactivation byproducts. According to this, clearly the water is removed when the temperature rises up to around 140°C; then reasonably we suspect that the thermolysis composition starts the nucleation of mineral phases which later form the composition of chemical inactivation admixture, a process which is completed around 230°C; then, the sludge transformation further continues over the temperature range from 140°C to 320°C case wherein the excess water and weakly bound water are continuously removed. It is expected the intercrystalline water is removed when the temperature is in the range from 320°C to 900°C, but this is also the temperature range wherein take place the chemical condensation of the intercrystalline bonding water, and hydroxo ligands of the various mineral speciations already nucleated in the sludge inactivation composition.

*Table 2*  
**The analytical results of leachability tests made at 250°C and 350°C**

Analyte	Measure unit	Results at 250°C	Results at 350°C	Reference
Dissolved organic carbon (DOC)	mg/kg SU	2420	970	[21]
pH	pH Unit	8.2	8.6	[22]
Electrical conductivity (25°C)	µS/cm	4900	2100	[22]
Chlorides	mg/kg SU	10200	3610	[23]
Fluorides	mg/kg SU	4.3	1.1	[24]

Solid residue at 105°C	mg/kg SU	30100	15500	[25]
Sulfate	mg/kg SU	8200	4900	[26]
Arsenic	mg/kg SU	0.133	0.075	[27]
Mercury	mg/kg SU	<0.00020	<0.00020	[28]
Barium	mg/kg SU	0.106	0.081	[29]
Cadmium	mg/kg SU	<0.006	<0.006	[29]
Chromium	mg/kg SU	0.942	0.035	[29]
Copper	mg/kg SU	0.458	0.127	[29]
Molybdenum	mg/kg SU	0.269	0.228	[29]
Lead	mg/kg SU	<0.051	<0.051	[29]
Selenium	mg/kg SU	<0.20	<0.20	[29]
Antimony	mg/kg SU	<0.10	<0.10	[29]
Zinc	mg/kg SU	0.66	<0.10	[29]
Nickel	mg/kg SU	0.676	<0.040	[29]

According to national environmental regulations specific to inert waste, the leaching permits for DOC, chlorides, and sulfates (when the liquid-to-solid ratio of 10 L/kg and particle sizes of inert waste materials are below 4 mm), are 500 mg/kg, 800 mg/kg, and 1000 mg/kg. From Table 2, we noticed that when the temperature rise from 250°C to 350°C, the amount of percolated DOC, chlorides, and sulfates, decrease with about 40, 35, respectively 60 percents on each about 100°C, wherein naturally we may assume these measured values are proportional with the increase of chemical inactivation rate. Hence, referencing the limits allowed by national permits for percolated values of the above mentioned leaching tests, we estimated the chemical inactivated sludge reaches the above mentioned allowed percolation limits to be disposed at temperature which is situated between 400°C and 500°C, and thus being expected that the amount of measured DOC, chlorides, and sulfates after percolation to decrease at about 156 mg/kg, 452 mg/kg, and 1750 mg/kg respectively.

Consistent with measurements presented in Table 2 and additionally, by comparing the amount of analytes leached from the sludge that was chemically inactivated at different temperatures, we note that the mobility of contaminants within the composition of chemically inactivated sludge significantly decreases when the temperature increases. The increase in pH when all other leaching parameters decrease may be explained by assuming that through rehydrating the composition of chemically inactivated sludge, small particles of basic salts may be formed, solubilized, or released during leaching, thus contributing to the rise in the level of total solid residues and dissolved organic carbon.

#### 4. Conclusions

The work presents one advanced solution for chemical inactivation and safe disposal of sludge produced after treating liquid waste. One advanced material that was previously reported is used for chemical inactivation of sludge under low-temperature thermolysis conditions.

The investigations made through DTA and DSC indicate the water evaporation endothermic effect prevails, and therefore, the chemical inactivation of after-treatment sludge passes through discrete transformations of particular aqua-oxo-hydroxylated phases into oxides. The experimental evidence provided by DTA and DSC is in excellent agreement with morpho-structural and XRD investigations we made, revealing that produced chemical inactivation byproducts comprise highly condensed oxo-hydrated materials phases of the main cations present in the sludge undergoing the thermolysis process.

Additionally, the FTIR investigations of chemically inactivated material indicate that one of the main mechanisms undertaking chemical inactivation of waste having complex contamination is chemical condensation which gives rise to new materials with reduced chemical functionality and high chemical stability, such as, for example, mineral oxysalts. The thermolysis byproducts comprise compounds with very limited chemical functionality consisting of only a few specific types of chemical functionalities which are bonded or encapsulated throughout the composition of the above-said highly condensed mineral oxysalts.

The leaching investigations made on the inactivation byproducts produced when the sludge is treated at 350°C show these completely fix the heavy metals and significantly reduce the level of dissolved organic carbon, sulfates, and fluorides, below 1000 mg/kg SU, 500 mg/kg SU, and 1 mg/kg SU respectively.

### Acknowledgements

Work made with government support under Grant number SMIS119960 awarded by the Romanian European Investments and Projects Ministry.

### R E F E R E N C E S

- [1]. *M.N. Yahyaa, H. Gökçekuş, and D.U. Ozsahin*, “A comparative assessment of intensive and extensive wastewater treatment technologies for removing emerging contaminants in small communities”, in *Water Res.*, **vol. 88**, Jan. 2016, pp. 777-785.
- [2]. *B. Wu, X. Dai, and X. Chai*, “Critical review on dewatering of sewage sludge: Influential mechanism, conditioning technologies and implications to sludge re-utilizations”, in *Water Res.*, **vol. 180**, August 2020, 115912.
- [3]. *A. J. Tóth, D. Fózér, P. Mizsey, P. S. Varbanov, and J. J. Klemeš*, “Physicochemical methods for process wastewater treatment: powerful tools for circular economy in the chemical industry”, in *Rev. Chem. Eng.*, **vol. 39**, 7, Aug. 29, pp. 1123-1151.
- [4]. *M. T. El-Saadony, A. M. Saad, N. A. El-Wafai, H. E. Abou-Aly, H. M. Salem, S. M. Soliman, T. A. Abd El-Mageed, A. S. Elrys, S. Selim, M. E. Abd El-Hack, S. Kappachery, K. A. El-Tarably, S. F. AbuQamar*, “Hazardous wastes and management strategies of landfill leachates: A comprehensive review”, in *Environ. Technol. Innov.*, **vol. 31**, Aug. 2023.
- [5]. *E. R. Bandala, A. Liu, B. Wijesiri, A. B. Zeidman, and A. Goonetilleke*, “Emerging materials and technologies for landfill leachate treatment: a critical review”, in *Environ. Pollut.*, **vol. 291**, Dec. 2021, 118133.
- [6]. *Yixia Chen, Mingwei Lin, and Dan Zhuang*, “Wastewater treatment and emerging contaminants: Bibliometric analysis”, in *Chemosphere*, **vol. 297**, June 2022, 133932.

- [7]. *N. Genç, E. D. Pişkin, and Ş. Aydin*, “Optimization of ZVAl based oxidation and reduction rocess conditions: Selection of the most suitable process by multiple-criteria decision-making approach”, in Process Saf. Environ. Prot., **vol. 159**, March 2022, pp. 605-615.
- [8]. *T. Fournie , T. L. Rashwan , C. Switzer , G. P. Grant , J. I. Gerhard*, “Exploring PCDD/Fs and potentially toxic elements in sewage sludge during smouldering treatment”, in J. Environ. Manage., **vol. 317**, Sept. 2022, 115384.
- [9]. *S. M. Lim , L. He, S. H. Goh, and F. H. Lee*, “Strength of Chemically Stabilized Sewage Sludge - Some Inferences from Recent Studies”, in Geotech., **vol. 1**, 2, Dec. 2021, pp. 573-587.
- [10]. *H. Malhotra, S. Kaur, and P. S. Phale*, “Conserved Metabolic and Evolutionary Themes in Microbial Degradation of Carbamate Pesticides”, in Sec. Microbiotechnology, **vol. 12**, July 2021.
- [11]. *P. Bhatt, X. Zhou, Y. Huang, W. Zhang, and S. Chen*, “Characterization of the role of esterases in the biodegradation of organophosphate, carbamate, and pyrethroid pesticides”, in J. Hazard. Mater., **vol. 411**, June 2021, 125026.
- [12]. *K. Kalkanis, D. E. Alexakis, E. Kyriakis, K. Kiskira, J. Lorenzo-Llanes, N. J. Themelis, and C. S. Psomopoulos*, “Transforming Waste to Wealth, Achieving Circular Economy”, in Circ.Econ.Sust., **vol. 2**, Nov. 2022, pp. 1541–1559.
- [13]. *T. Mester ,G. Szabó,Z. Sajtos,E. Baranyai,G. Szabó, and D. Balla*, “Environmental Hazards of an Unrecultivated Liquid Waste Disposal Site on Soil and Groundwater”, in Water, **vol. 14**, 2, Jan. 2022, 226.
- [14]. *Sh. Yeilagi, S. Rezapour, and F. Asadzadeh*, “Degradation of soil quality by the waste leachate in a Mediterranean semi-arid ecosystem”, in Sci. Rep., **vol. 11**, May 2021, 11390.
- [15]. *J. Rumky, A. Deb, M. J. Shim, E. Laakso, and E. Repo*, “A review on the recent advances in electrochemical treatment technologies for sludge dewatering and alternative uses”, in JHM Advances, **vol. 11**, Aug. 2023, 100341.
- [16]. *L. Bretschger, and K. Pittel*, “Twenty Key Challenges in Environmental and Resource Economics”, in Environ. Resource Econ., **vol. 77**, October 2020, pp. 725–750.
- [17]. *D. Scrinzi, R. Ferrentino, E. Baù, L. Fiori, and G. Andreottola*, “Reduction and Nutrients Recovery via Hydrothermal Carbonization”, in Waste Biomass Valor., **vol. 14**, October 2022, pp. 2505–2517.
- [18]. *R. Chen, Q. Sheng, X. Dai, and B. Dong*, “Upgrading of sewage sludge by low temperature pyrolysis: Biochar fuel properties and combustion behavior”, in Fuel, **vol. 300**, Sept. 2021.
- [19]. *O. D. Alupei-Cojocariu, A. Banu, M. R. Dijmărescu, D. Ş. Preda, E. Rusu, and P. Z. Iordache*, “Green aqua-oxo-hydroxylated advanced materials for treatment of liquid waste with complex contamination”, in UPB Sci. Bull. B: Chem. Mater., **vol. ....**, Dec. 2023.
- [20]. *K. I. Hadjiivanov, D. A. Panayotov, M. Y. Mihaylov, E. Z. Ivanova, K. K. Chakarova, S. M. Andonova, and N. L. Drenchev*, “Power of Infrared and Raman Spectroscopies to Characterize Metal-Organic Frameworks and Investigate Their Interaction with Guest Molecules”, in Chem. Rev., **vol. 121**, 3, Dec. 2020, pp. 1286-1424.
- [21]. *W-DOCPHOS10, Analytical investigation method used for assessment*, SR EN 12457-2:2003, Waste characterization. LEACHING. Characterisation of waste - Leaching - Compliance test for leaching of granular waste materials and sludges - Part 2: One stage batch test at a liquid to solid ratio of 10 l/kg for materials with particle size below 4 mm (without or with size reduction), SR CEN/TS 16192:2020, ISO 15705:2002 Water quality. Determination of chemical oxygen consumption. The colorimetric method in a closed tube.
- [22]. *I-PPL24-S10, Analytical investigation method used for assessment*, PSL-25, SR EN 12457-2:2003, Characterisation of waste - Leaching - Compliance test for leaching of granular waste materials and sludges - Part 2: One stage batch test at a liquid to solid ratio of 10 l/kg for materials with particle size below 4 mm (without or with size reduction).
- [23]. *W-CLSPGS10, Analytical investigation method used for assessment*, PSL-54, SR EN 12457-2:2003 Waste characterization. LEACHING. Characterisation of waste - Leaching - Compliance test for leaching of granular waste materials and sludges - Part 2: One stage batch test at a liquid

to solid ratio of 10 l/kg for materials with particle size below 4 mm (without or with size reduction). SR CEN/TS 16192:2020; ISO 15923:2013 Water quality. Determination of parameters through a discrete analysis system, 44.

[24]. *W-FSPGS10, Analytical investigation method used for assessment*, SR EN 12457-2:2003 Waste characterization. LEACHING. Characterisation of waste - Leaching - Compliance test for leaching of granular waste materials and sludges - Part 2: One stage batch test at a liquid to solid ratio of 10 l/kg for materials with particle size below 4 mm (without or with size reduction). SR CEN/TS 16192:2020; ISO 15923:2013 Water quality. Determination of parameters through a discrete analysis system, 44.

[25]. *W-TDSGRS10, Analytical investigation method used for assessment*, SR EN 12457-2:2003 Waste characterization. PSL-31, SR EN 12457-2:2003 Waste characterization. LEACHING. Characterisation of waste - Leaching - Compliance test for leaching of granular waste materials and sludges - Part 2: One stage batch test at a liquid to solid ratio of 10 l/kg for materials with particle size below 4 mm (without or with size reduction). SR CEN/TS 16192:2020, SR EN 15216:2008, STAS 9187-84 (cap. 6) Determinarea reziduului filtrabil; 10.

[26]. *W-SO4SPGS10, Analytical investigation method used for assessment*, SR EN 12457-2:2003 Waste characterization. PSL-54, SR EN 12457-2:2003 Waste characterization. LEACHING. Characterisation of waste - Leaching - Compliance test for leaching of granular waste materials and sludges - Part 2: One stage batch test at a liquid to solid ratio of 10 l/kg for materials with particle size below 4 mm (without or with size reduction). SR CEN/TS 16192:2020, ISO 15923:2013 Water quality. Determination of parameters through a discrete analysis system, 44.

[27]. *W-METDGS10, Analytical investigation method used for assessment*, SR EN 12457-2:2003 Waste characterization. PSL-24, SR EN 12457-2:2003 Waste characterization. LEACHING. Characterisation of waste - Leaching - Compliance test for leaching of granular waste materials and sludges - Part 2: One stage batch test at a liquid to solid ratio of 10 l/kg for materials with particle size below 4 mm (without or with size reduction). SR CEN/TS 16192:2020, SR EN ISO 11885:2009, SR EN ISO 15587-2:2003 The assessment of selected elements by spectroscopy of inductively coupled plasma optical emission (ICP-OES). Mineralization for the determination of some elements in water. Part 2: Nitric acid mineralization (The sample was homogenized and mineralized with nitric acid in an autoclave under high pressure and temperature before analysis; 41.

[28]. *W-HGDGS10, Analytical investigation method used for assessment*, CZ\_SOP\_D06\_02\_096 (US EPA 245.7, CSN EN ISO 178 52, CSN EN 16192, sample preparation according to CZ\_SOP\_D06\_02\_J02 chap. 10.1 and 10.2.). The assessment of Mercury by Fluorescence Spectrometry. The results are calculated in mg/kg SU for a 10/1 leaching ratio.

[29]. *W-METDGS10, Analytical investigation method used for assessment*, PSL-24, SR EN 12457-2:2003 Waste characterization. LEACHING. Characterisation of waste - Leaching - Compliance test for leaching of granular waste materials and sludges - Part 2: One stage batch test at a liquid to solid ratio of 10 l/kg for materials with particle size below 4 mm (without or with size reduction). SR CEN/TS 16192:2020, SR EN ISO 11885:2009, SR EN ISO 15587-2:2003 The assessment of selected elements by spectroscopy of inductively coupled plasma optical emission (ICP-OES). Mineralization for the determination of some elements in water. Part 2: Nitric acid mineralization (The sample was homogenized and mineralized with nitric acid in an autoclave under high pressure and temperature before analysis; 41.